Mars and Mercury rotation variations from altimetry crossover data: Feasibility study

Séverine Rosat, P. Rosenblatt, A. Trinh, V. Dehant

Mars and Mercury rotation variations from altimetry crossover data: Feasibility study

S. Rosat,[1,2] P. Rosenblatt,[1] A. Trinh,[1] and V. Dehant[1]

Received 4 July 2008; revised 29 September 2008; accepted 20 October 2008; published 30 December 2008.

[1] Knowledge of the interior structure of terrestrial planets can be achieved by studying the changes of their rotation and orientation in time. We simulate the use of time deviations of altimetry crossover positions to infer information on the nutations of Mars and on the librations of Mercury. The analysis is based on the least squares estimator and uses simulated crossover points. The simulations demonstrate that the use of crossover data improves the estimates of the observed libration amplitude and obliquity of Mercury and allows detecting the nutations of Mars.

Citation: Rosat, S., P. Rosenblatt, A. Trinh, and V. Dehant (2008), Mars and Mercury rotation variations from altimetry crossover data: Feasibility study, *J. Geophys. Res.*, *113*, E12014, doi:10.1029/2008JE003233.

1. Introduction

[2] Knowledge of the interior structure of terrestrial planets can be achieved by studying the changes of their rotation and orientation in time. In this article, we focus on the planets Mars and Mercury. Two missions have been scheduled to orbit Mercury: the MESSENGER mission [*Solomon et al.*, 2007], launched on 3 August 2004 and foreseen to be inserted into Mercury orbit on March 18th 2011, and the future BepiColombo (BC) mission [*Anselmi and Scoon*, 2001], which is foreseen for launch in August 2013 with an arrival at Mercury in August 2019. Both missions have onboard laser altimeter called MLA (Mercury Laser Altimeter) and BELA (BEpiColombo Laser Altimeter [*Thomas et al.*, 2007]), for MESSENGER and BepiColombo missions, respectively. The interdisciplinary BepiColombo mission consists of two spacecrafts, Mercury Magnetospheric Orbiter (MMO), which is dedicated to the study of the planet and its environment, and the Mercury Planetary Orbiter (MPO), which has the BELA instrument onboard. The laser altimeter will scan Mercury's surface for about one year in order to measure the shape of the planet with an accuracy of 10 m and the topography with an accuracy of 1 m with a grid spacing of a few hundred meters cross-track. The characteristics of the planned MPO orbit are summarized in Table 1.

[3] The Mars Global Surveyor (MGS) spacecraft was equipped with a laser-altimeter called MOLA (Mars Orbiter Laser Altimeter [*Zuber et al.*, 1992]) that scanned Mars' surface during 3 years. The ground tracks of the laser-shots often cross because of the rotation of Mars and the evolving orbit of MGS. Therefore the position of the crossing points projected on the surface of the planet contains information on the rotation of Mars and on the spacecraft orbit. In particular, the spacecraft orbit is not exactly known because of imperfections in the knowledge of Mars' gravity field and its variations, of Mars' varying rotation, and of other phenomena such as imperfections in the modeling of the atmospheric drag on the spacecraft or of the inertial wheel desaturation amplitudes etc. Therefore, by using differences in altimetry measurements (radial differences) at crossovers, it was possible to constrain the MGS orbit and hence Mars' gravity field and topography [e.g., *Neumann et al.*, 2001].

[4] In this article, we study the possibility to use the information embedded in the MOLA and BELA crossing ground tracks in order to determine the rotation variations of Mars and Mercury. In particular, we investigate the possibility that the time evolution of the surface crossover positions (i.e., tangential differences) can help us to detect the nutations of Mars, to improve the determination of the Martian length-of-day (LOD) variations (spin rate), to detect the librations of Mercury and to improve the determination of Mercury's obliquity. For that purpose, we have first simulated crossing ground tracks by using MGS and MPO orbital characteristics (Table 1) and a model of the rotation of Mars based on the results from *Konopliv et al.* [2006] and of the rotation of Mercury using the observed values of longitude libration and obliquity by *Margot et al.* [2007]. Then, we have considered the inverse problem solved by a least-square fit based on the theory of *Tarantola and Valette* [1982], where the parameters are the amplitudes of the angles of the rotation model and the data are the crossover coordinates ("geo"graphic longitude and latitude), derived from the simulated crossing ground tracks. Section 2 shows the altimetry precision with respect to the investigated signals. Sections 3 and 4 describe the rotation model of Mars and Mercury, respectively. The results of our simulations are presented in section 5 and discussed in section 6.

2. Altimetry Precision and Amplitudes of the Investigated Signals

[5] In the MGS mapping orbit, the instrument's 10-Hz sampling rate combined with the laser beam divergence of

[1]Department Reference Systems and Geodynamics, Royal Observatory of Belgium, Brussels, Belgium.
[2]Now at Ecole et Observatoire des Sciences de la Terre-Institut de Physique du Globe de Strasbourg, Strasbourg, France.

0148-0227/08/2008JE003233

Table 1. Mars Global Surveyor and BepiColombo Spacecraft Orbit Characteristics

Orbit Parameters	MGS	BepiColombo
Altimeter	MOLA	BELA
Orbit period	1.96 h	2.32 h
Repeatability (error)	7 Days, 88 revolutions (0.08%)	1 Day, 607 revolutions (0.04%)
Inclination	92.87 deg	89.5 deg
Uncertainty (100 m) to planet radius	2.95×10^{-5}	4.1×10^{-5}
Number of crossovers during the repeatability period (after filtering)	5428	21,340

0.4 mrad results in a surface spot size of 160 m and shot-to-shot spacing of 330 m. The precision of MOLA range measurements approaches the limiting resolution of 37.5 cm on smooth level surfaces and may increase up to 10 m on 30° slopes [*Smith et al.*, 1999]. The accuracy of the spot location in latitude and longitude is limited by the knowledge of the spacecraft pointing at 1 to 3 mrads (400 to 2000 m on the surface, depending on the spacecraft altitude) and spacecraft position uncertainties of a few hundred meters. So the spacecraft pointing error dominates the total error budget. After correction for orbit and pointing errors, *Neumann et al.* [2001] demonstrated that the horizontal position accuracy on Mars' surface can decrease to 100 m. They have used a linear basis of polynomial functions fitted once or twice per revolution in order to correct for the attitude errors when there was no constraint from tracking. Note that some attitude errors that can be thermally driven are non-stochastic; so they are not simply solved by a periodic correction once per revolution term.

[6] In the BC mapping orbit, the tracking accuracy is expected to be a few decimeters and the spacecraft pointing accuracy should be less than 0.5 mrad to reach meter-scale altitude precision [*Thomas et al.*, 2007]. The BELA footprint size is expected to reach about 20 m from 400 km altitude. As for MGS, we can expect to reach a horizontal position accuracy of 100 m after correction for the orbit and pointing errors. The MOLA and BELA accuracies are summarized in Table 2.

[7] The signals that we are investigating are the nutations of Mars with amplitude up to 1000 milliarcsecond (mas), i.e., 16 m on the surface, and the length-of-day variations with an amplitude of about 400 mas, i.e., 7 m displacement on the surface. For Mercury, we are looking for the libration in longitude, of which the amplitude is about 36,000 mas, corresponding to about 425 meters on the surface [*Margot et al.*, 2007]. We also investigate the obliquity of Mercury, which has observed amplitude of 2.11 arc min or 1.5 km on Mercury's surface [*Margot et al.*, 2007].

[8] Mercury's librations in longitude and obliquity have much larger amplitudes than the expected accuracy for these quantities with the BepiColombo mission. However, the MPO spacecraft is foreseen to have a polar orbit and because of the slow rotation of Mercury, the number of crossing tracks will be small at mid latitudes. For the nutations of Mars, the investigated signal has smaller amplitude (less than 20 m) than the position accuracy (100 m), so that the corrections for orbit and pointing errors are fundamental. Fortunately, there are a huge number of crossovers that perfectly cover the whole surface of Mars. Statistically, supposing a Gaussian distribution, with an uncertainty decreasing by $\sqrt{(N)}$ where N is the number of laser shots, we need 100 altimetry laser measurements in order to reach a 10 m-accuracy. For the laser footprint size of MOLA, assuming a foot size of 160 m, we need 256 altimetry shoots in order to decrease the error to 10 m. On the other hand, for a feasibility study, orbital solution errors may be ignored, as they are treated separately in the tracking data solution.

[9] Besides being a slow rotator, Mercury experiences significant m-level daily tidal perturbations, which will cause perturbations in the eccentricity and inclination of its orbit [*Kaula*, 1966]. These tidal effects will also change the spatial distribution of the crossover. The radial perturbation due to the tides of the altimetry measurement is expected to be about 40 m [*Trinh*, 2007] and the horizontal shift of the ground track about 25 m at the equator. These perturbations are usually taken into account in the tracking process using radioscience as well as the daily periodic effects of the second-degree harmonics of the gravity field on the spacecraft position. In altimetry, one uses an instantaneous orbit which includes all these effects. We suppose that the remaining tidal or gravity effect due to their mis-modeling will be negligible. Therefore, in the simulation, we do not take these effects into account.

3. Mars Orientation Model

[10] The transformation between the position of the spacecraft in the Mars body-fixed system $\vec{r}_{bf}$ and the inertial position $\vec{r}_{in}$ in the Earth mean orbit for epoch

Table 2. Accuracy of the MGS and BC Orbits and Precision of the MOLA and BELA Altimeters

Mission-Spacecraft	MGS	BepiColombo-MPO
Altimeter	MOLA	BELA
Orbit accuracy	1.7 (tracked)–10 m	10 cm (tracked)–3 m
Laser pointing uncertainty	1–3 mrad [*Smith et al.*, 1999] 0.42 mrad (210 m) [*Rowlands et al.*, 1999] using crossovers	Should be <0.5 mrad
Laser footprint size	70–300 m (120 m from 400 km altitude)	~20 m from 400 km altitude
Horizontal position accuracy after orbit and pointing corrections	100 m [*Neumann et al.*, 2001]	Expected <100 m

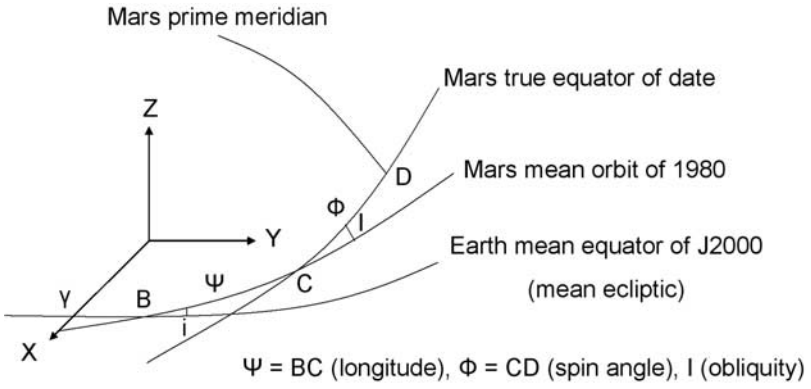

Figure 1. Definition of the Mars orientation angles for conversion between the Earth mean orbit of J2000 and the Mars body-fixed coordinates. The angles are similar to define Mercury's orientation.

J2000 system is given by a series of rotation [e.g., *Folkner et al.*, 1997]:

$$\vec{r}_{in} = R_z(-\psi)R_x(-I)R_z(-\phi)R_y(X_p)R_x(Y_p)\vec{r}_{bf}, \qquad (1)$$

where the angles are shown in Figure 1. The angle ψ is the angle from the node of the Mars mean orbit and Earth's mean orbit of J2000 (or mean ecliptic) to the node of the Mars true equator of date and the Mars mean orbit for epoch 1980. The angle I is the inclination of the Mars true equator of date relative to the Mars mean orbit. The angle ϕ is the spin angle from the node of the Mars true equator of date and Mars mean orbit to the prime meridian of Mars. The angles X_p and Y_p correspond respectively to the body-fixed x and y components for the polar motion (not shown in Figure 1), of which the amplitude is small, at a couple of meters level.

[11] The variation of the rotation of Mars can be decomposed into nutation, precession and spin rate variations inducing length of day (LOD) variations.

[12] The nutation of Mars affects the angles ψ and I, which can be written as

$$\psi(t) = \psi_0 + \dot{\psi}_0 t + \psi_{nut},\ I(t) = I_0 + \dot{I}_0 t + I_{nut}, \qquad (2)$$

where the terms ψ_{nut} and I_{nut} refer to the nutation contributions, t equals the time elapsed since the J2000 epoch, ψ_0 and I_0 are constant angles at J2000, $\dot{\psi}_0$ is a constant equal to the precession rate of Mars and $\dot{I}_0$ is a constant equal to the secular change in the Mars obliquity (orbit inclination) relative to the Mars mean orbit of epoch 1980. The nutation contributions in longitude and obliquity are given by [*Reasenberg and King*, 1979]:

$$\psi_{nut} = \sum_{m=1}^{9} \psi_{m0} \sin(\alpha_m t + \theta_m) \text{ and}$$
$$I_{nut} = I_{00} + \sum_{m=1}^{9} I_{m0} \cos(\alpha_m t + \theta_m), \qquad (3)$$

where I_{00} is a small constant correction to the nutation in obliquity (difference between J1980 and J2000). The coefficients α_m and θ_m are expressed as functions of the Mars mean motion n' and the Mars mean anomaly at J2000 l'_0 by:

$$\alpha_m = \begin{cases} mn' & \text{for } m = 1,2,3 \\ (m-3)n' & \text{for } m = 4,5,\ldots 9 \end{cases} \text{ and}$$
$$\theta_m = \begin{cases} ml'_0 & \text{for } m = 1,2,3 \\ (m-3)l'_0 + q & \text{for } m = 4,5,\ldots 9 \end{cases},$$

where $q = 2w$ and w is the argument of perihelion of the Mars orbit relative to the node of the Mars equator and the Mars mean orbit at the epoch J2000. The angle $q = 142°$.

[13] *Konopliv et al.* [2006] have introduced a slight modification of Reasenberg and King's nutation model by introducing small corrections to the nutation amplitudes ψ_{m0} and I_{m0} for a Mars fluid core. Since these corrections are too small with respect to the uncertainties on the nutation amplitudes, we do not consider them in a first analysis. A more recent evaluation of the nutation amplitudes by *Roosbeek* [2000] provides values very close to the Reasenberg and King's model. The reference epoch considered in Roosbeek is J2000. The position of the mean equator of Mars at that epoch is provided in the study by *Seidelmann et al.* [2002]. The differences between these two models are also too small with respect to the uncertainties. The components $m = 3$ and $m > 6$ are not considered because of their smaller amplitudes.

[14] The spin angle ϕ is defined as

$$\phi(t) = \phi_0 + \dot{\phi}_0 t + \sum_{j=1}^{4} \left(\phi_{cj}\cos(jl') + \phi_{sj}\sin(jl')\right), \qquad (4)$$

where ϕ_0 is a constant at J2000, $\dot{\phi}_0$ is the Mars spin rate and l' is the Mars mean anomaly. The constants ϕ_{cj} and ϕ_{sj} are amplitudes of periodic terms in spin corresponding to the LOD variations. We consider only the annual and semi-annual components, which are the largest variations of the spin angle.

[15] Polar motion is decomposed into an annual and a semi-annual oscillation for both the x and y components. We also add the Chandler-Wobble (CW, with a period

Table 3. Mars Orientation Parameters From *Konopliv et al.* [2006] and Mercury Orientation Parameters From *Balogh and Giamperi* [2002] and *Margot et al.* [2007] for the Obliquity

Orientation Parameter at J2000	Mars	Mercury
l'_0 (mean anomaly)	19.387 deg	174.796 deg
n' (mean motion)	687 days	87.969 days
ψ_0 (node longitude)	81.968 deg	48.331 deg
$\dot{\psi}_0$ (precession rate)	$-5.756\ 10^{-6}$ deg/day	$-4.197\ 10^{-6}$ deg/day
I_0 (obliquity)	25.189 deg	2.1 ± 0.1 arcmin (0.035 ± 0.0017 deg)
$\dot{I}_0$ (secular change in obliquity)	$5\ 10^{-9}$ deg/day	0
ϕ_0 (spin angle)	133.385 deg	0 (arbitrary)
$\dot{\phi}_0$ (spin rate)	350.892 deg/day	6.1 deg/day

chosen to 205 days [*Van Hoolst et al.*, 2000a]) x and y components:

$$Xp = Xp_{1c}\cos(n't) + Xp_{1s}\sin(n't) + Xp_{2c}\cos(2n't) + Xp_{2s}\sin(2n't) + X_{CWc}\cos(3.34n't) + X_{CWs}\sin(3.34n't) \quad (5)$$

$$Yp = Yp_{1c}\cos(n't) + Yp_{1s}\sin(n't) + Yp_{2c}\cos(2n't) + Yp_{2s}\sin(2n't) + Y_{CWc}\cos(3.34n't) + Y_{CWs}\sin(3.34n't) \quad (6)$$

[16] We use the values given by *Konopliv et al.* [2006] for the orientation parameters and the values from *Reasenberg and King* [1979] for Mars' nutation amplitudes. These values are summarized in Tables 3 and 4. Mars' seasonal spin amplitudes have been computed by *Konopliv et al.* [2006] using the MGS95J gravity solution. The given LOD variations come primarily from the Viking and Pathfinder Lander data. The values for the annual and semi-annual polar motion amplitudes are taken from *Van den Acker et al.* [2002] and *Konopliv et al.* [2006] for the Chandler Wobble.

Table 4. The 27 MOP That are Modeled

Name	Frequency	Theoretical/Estimated Amplitude (mas)	Additional Data
		Nutations in Longitude: 5 Parameters	
ψ_{10}	Annual	−632.6	*Reasenberg and King* [1979]
ψ_{40}	Annual	−104.5	
ψ_{20}	Semi-annual	−44.2	
ψ_{50}	Semi-annual	1097.0	
ψ_{60}	Ter-annual	240.1	
		Nutations in Obliquity: 6 Parameters	
I_{00}	Constant	−1.4	*Reasenberg and King* [1979]
I_{10}	Annual	−0.4	
I_{20}	Semi-annual	0	
I_{40}	Annual	−49.1	
I_{50}	Semi-annual	515.7	
I_{60}	Ter-annual	112.8	
		Rotation Rate: 4 Parameters	
ϕ_{c1}	Annual	398 ± 31	MGS95J gravity solution from
ϕ_{s1}	Annual	−222 ± 41	*Konopliv et al.* [2006].
ϕ_{c2}	Semi-annual	−110 ± 31	
ϕ_{s2}	Semi-annual	−128 ± 30	
		Polar Motion (X): 6 Parameters	
Xp_{1c}	Annual	1.927 ± 5	*Van den Acker et al.* [2002] (atmospheric data)
Xp_{1s}	Annual	−2.031 ± 5	
Xp_{2c}	Semi-annual	−7.715 ± 5	
Xp_{2s}	Semi-annual	4.437 ± 5	
X_{CWc}	Chandler Wobble	5 ± 3	*Konopliv et al.* [2006], the uncertainties are
X_{CWs}	Chandler Wobble	5 ± 3	5 times the formal errors.
		Polar Motion (Y): 6 Parameters	
Yp_{1c}	Annual	−5.619 ± 5	*Van den Acker et al.* [2002] (atmospheric data)
Yp_{1s}	Annual	−10.263 ± 5	
Yp_{2c}	Semi-annual	−3.867 ± 5	
Yp_{2s}	Semi-annual	−0.509 ± 5	
Y_{CWc}	Chandler Wobble	5 ± 3	*Konopliv et al.* [2006], the uncertainties are
Y_{CWs}	Chandler Wobble	5 ± 3	5 times the formal errors.

Table 5. The 3 HOP That are Investigated

Name	Frequency	Theoretical Amplitude (mas)	Uncertainty	Additional Data
		Obliquity: 1 Parameter		
I_0		2.1 arcmin	0.1 arcmin	*Margot et al.* [2007] 1σ-uncertainty
		Libration: 2 Parameters		
γ_1	Annual	35,800	2000 mas	*Margot et al.* [2007]
$\gamma_2 = \gamma_1/K$	Semi-annual	−3775	2000 mas	$K = -9.483$ *Jehn et al.* [2004]

[17] The Mars Orientation Parameters (MOP) are given in Table 3 and the investigated ones in Table 4.

4. Mercury Orientation Model

[18] Mercury's rotation model can be defined in a way similar to that for Mars:

$$\vec{r}_{in} = R_z(-\psi)R_x(-I)R_z(-\phi)\vec{r}_{bf}, \tag{7}$$

where the angles ψ, I and ϕ have similar definitions as for Mars' rotation model. The polar motion of Mercury is negligible, so we have not considered it in our model.

[19] Because of the small effect of the nutations of Mercury compared to the 88-day libration, we also neglect them. The libration does not affect the obliquity [*Yseboodt and Margot*, 2006]. Hence the longitude and obliquity of Mercury can be written:

$$\psi(t) = \psi_0 + \dot{\psi}_0 t,\ I(t) = I_0 + \dot{I}_0 t, \tag{8}$$

where ψ_0 and I_0 are angle constant at J2000, $\dot{\psi}_0$ is a constant equal to the precession rate of Mercury and $\dot{I}_0$ is a constant equal to the secular change in the Mercury obliquity.

[20] The spin angle ϕ of Mercury is defined by:

$$\phi(t) = \phi_0 + \dot{\phi}_0 t + \gamma(t), \tag{9}$$

where ϕ_0 is a constant at J2000 and $\dot{\phi}_0$ is the Mercury spin rate. The 88-day forced libration in longitude γ can be expressed by [*Jehn et al.*, 2004]:

$$\gamma(t) = \gamma_1 \sin\left(n' t + l'_0\right) + \gamma_2 \sin\left(2n' t + 2l'_0\right), \tag{10}$$

where n' is Mercury mean motion and l'_0 is the Mercury mean anomaly at J2000. Their values are given in Table 3. γ_1 and γ_2 are the annual and semi-annual libration amplitudes.

[21] *Peale et al.* [2002] and *Yseboodt and Margot* [2006] have shown that Mercury's obliquity for Cassini state should be between 1.2 and 2.9 arc min (or 0.02 and 0.05°) based on the range of values provided by the Mariner 10 gravity data and the C/MR^2 (the normalized moment of inertia where M is the mass and R the radius of the planet) values encompassing all plausible interior models [*Harder and Schubert*, 2001; *Rambaux et al.*, 2007]. Recently, *Margot et al.* [2007] have measured an obliquity of 2.11 ± 0.1 arc min and observed a large longitude libration of 35.8 ± 2 arc seconds from radar echoes from the Mercury surface. Mercury's orientation parameters (or Hermean Orientation Parameters, HOP) are given in Table 3. The other values have been taken from *Balogh and Giamperi* [2002]. The a priori libration amplitudes are given in Table 5. Because of the small value of Mercury's obliquity and its small secular variation over the mission lifetime, we set $\dot{I}_0$ to zero.

[22] From these definitions of Mars and Mercury orientation models, we can now compute the altimetry crossover grids and perform the least-squares analysis.

5. Altimetry Crossover Analysis

[23] Our data are the crossover positions obtained using an a priori rotation model and relocated on the planet's surface using the observed slopes, altimetry residual and a static topography model. A perfectly smooth planet would not allow a crossover analysis to be attempted. Indeed, on a smooth, flat surface, the crossover residual provides no information about the actual location, as a lateral shift of either track does not change the altitude at the crossover. On a rough surface, the crossover residuals at multiple crossings will constrain the position of ground tracks. The strategy is therefore to match the tracks to some specific features like in the Tharsis region where the topography is highly varying.

[24] As the orbital period of MGS is 1.96 h and the revolution period of Mars is 24.62 h, the repeatability period of MGS is 7 days corresponding to 88 MGS revolutions, as 24.62/1.96 ≈ 88/7 with a relative error of 0.08%. For Mercury, the sidereal period is 1407.6h while the BepiColombo orbital period is planned to be 2.32h, leading to a repeatability period of 1 Hermean day for 607 revolutions of BepiColombo with an error of 0.04% (1407.6/2.32 ≈ 607).

[25] An example of crossover distribution on Mars' surface after 20 revolutions of MGS is represented in Figure 2. Notice the good coverage of crossover points. Because of the slow rotation of Mercury and the polar orbit of the MPO spacecraft (90 ± 0.1°), the number of ground track crossings is limited. The ground tracks are parallel until the 304th revolution, when Mercury has performed half a revolution (Figure 3a). After 607 revolutions of the MPO spacecraft, the BELA ground tracks cross only in some well-limited areas (Figure 3b, white segments) around ±24.83°. In such a situation, the crossovers are badly distributed on Mercury's surface, so their information on Mercury's rotation will be restricted. However, we can expect that the actual inclination of the MPO orbit will not be exactly 90°, which would improve the situation. In the following, we assume an orbit inclination of 89.5°. The corresponding ground tracks and the generated crossovers after 607 revolutions are represented in Figure 3c. In this case, the crossover distribution is still not homogeneous on the surface, especially in latitude, though there are more

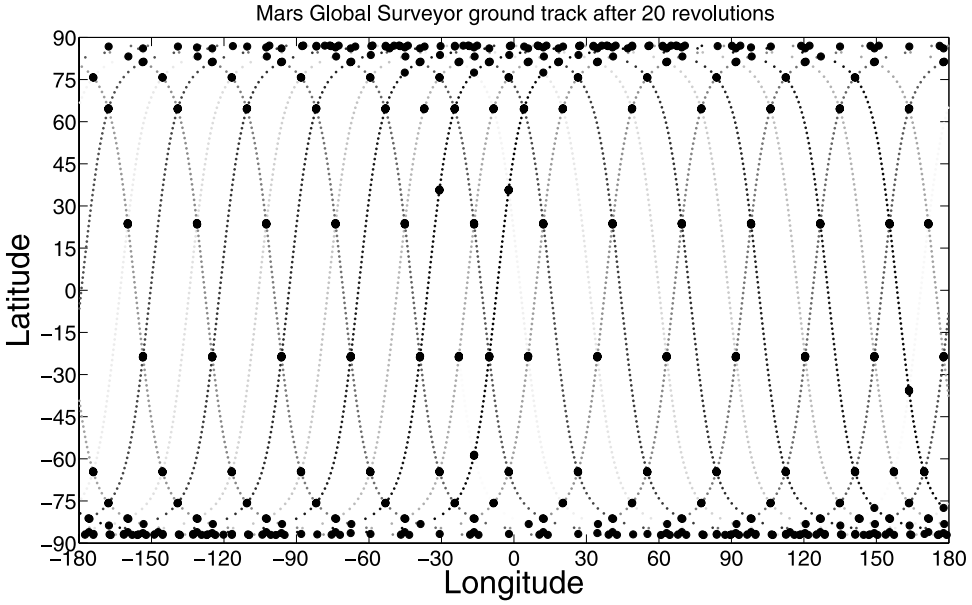

Figure 2. Mars Global Surveyor ground tracks and crossovers after 20 revolutions around Mars.

crossover points. We will see that this improvement is sufficient to recover the large obliquity and libration.

[26] We consider a grid of crossover point coordinates during the repeatability period of 7 days for Mars and 1 day for Mercury and we compute the displacement of these crossovers in inertial space, based on the rotation models presented in sections 2 and 3. The difference between the simulated grid of crossovers and the a priori crossover grid coordinates in an inertial space based on a priori rotation parameters is then minimized in a least-square inversion problem as in the study by *Tarantola and Valette* [1982]. The solution leads to the a posteriori rotation parameters that best fit the simulated crossover grid location. We have used a value of 100 m for the standard deviation of each crossover position in longitude and in latitude [*Zuber et al.*, 1992; *Neumann et al.*, 2001] for MOLA, as well as for BELA. This formal uncertainty is rather optimistic as the possible correlation between crossovers is not considered. In addition, the actual location of crossovers cannot be known with uniform uncertainty, since their position can only be well constrained when the surface is rough. In practice using actual data, each crossover position at the planetary surface cannot be determined using only the ground track projection obtained from a given rotation model, but also needs to use the topography of the planetary surface (which can be determined from the whole set of data, smoothing out the time variations of the topography induced by the nutations or librations or length-of-day variations). For determining the crossover positions, the slopes along the azimuths of the 2 crossing tracks and the altimetric residual at each crossover are used to estimate the associated topographic position. The shift between the positions estimated from a given rotation model and from the topography could be interpreted in terms of a periodic rotation of the planet; as the topography of the planet was estimated from taking the mean of altimetry measurements, all the periodic signals which we are looking for (nutations, spin rate, librations, ...) have been cancelled in the averaging process. Consequently, the meaningful data are distances between the crossover locations estimated from the ground tracks projection with a given rotation model and the actual topographic positions corresponding to the observed slopes in the two track azimuths. The crossovers that will provide the most useful information are those obtained on a very rough surface. For Mars, they are the points located mainly between latitudes $-40°$ and $40°$, especially close to the volcanoes of Tharsis. Therefore, in the simulation, we will also use only a group of crossovers located around the Tharsis region (at latitudes between 40 and $-40°$, and longitudes between $-150°$ and $50°$). Moreover, at such latitudes for Mars, we avoid altimetric variations induced by the seasonal CO_2 deposits at polar caps.

[27] The covariance matrix of the model parameters of the inverse problem $d = G\ p$ can be written as follows [*Tarantola and Valette*, 1982]:

$$C_{pp} = \left(G^T C_{d0d0}^{-1} G + C_{p0p0}^{-1} \right), \tag{11}$$

where C_{p0p0} are the a priori constraints on the parameters. We set C_{p0p0} to be a diagonal matrix of the prior uncertainties on the parameters. The a priori uncertainties

Table 6. Results of the Global Inversion of MOP Using the Simulated Crossovers During One Repeatability Period of MGS[a]

A Priori Model (mas)	Perturbation Applied on the Model (mas)	A Posteriori Uncertainty (mas)
	Nutation in Longitude	
	Estimated annual and semi-annual amplitude	
0 ± 2000	ψ_{50} = 1089	144
0 ± 1000	ψ_{60} = 155	130
	Nutation in Obliquity	
	Estimated annual and semi-annual amplitude	
0 ± 1000	I_{50} = 514	99

[a]We have taken large a priori uncertainties for the nutation amplitudes because they have never been observed.

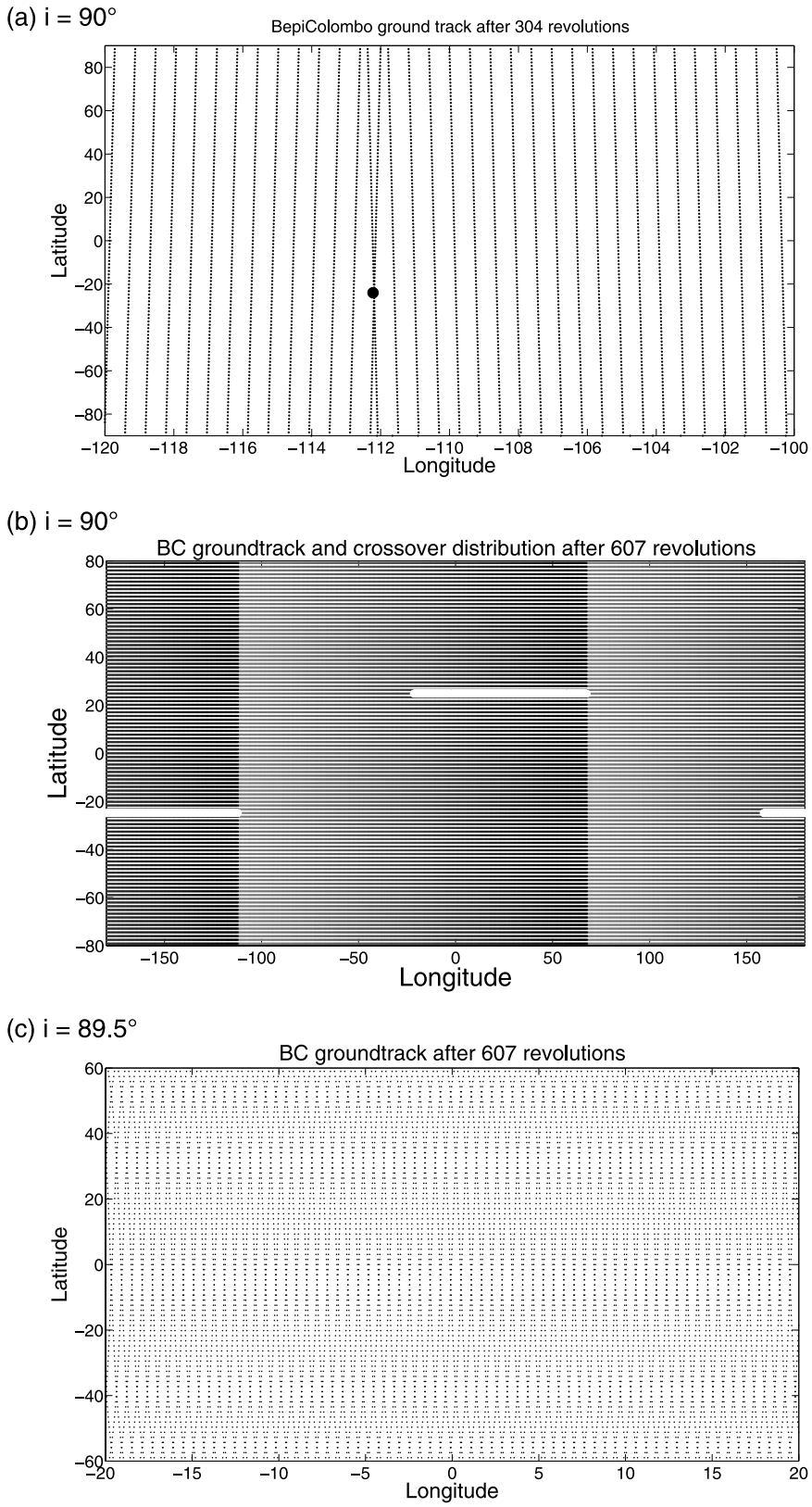

Figure 3. BepiColombo ground tracks and crossover distribution (a) after 304 revolutions and (b) after 607 revolutions around Mercury with an orbit inclination of 90°. The tracks do not cross before the 304th revolution of BC around Mercury. This first crossover is indicated by a large point. After 607 revolutions, the crossover locations are concentrated around ±24.83° in latitude and are represented on the map by the white bands. (c) BC ground tracks with an orbit inclination of 89.5° after 607 revolutions around Mercury. The crossing tracks are better distributed.

Table 7. Results of the Global Inversion of HOP Using the Simulated Crossovers During One Repeatability Period of MPO

A Priori Model	Perturbation Applied on the Model	A Posteriori Error
	Obliquity	
	Estimated value	
0 ± 6 arcmin	I_0 = 2.1 arcmin	< 0.001 arcmin
	Libration	
	Estimated annual and semi-annual amplitudes	
0 ± 2000 mas	γ_1 = 35709 mas	100 mas
0 ± 2000 mas	γ_2 = −3766 mas	100 mas
	K = −9.5	0.3

on the nutation/libration amplitudes have been taken very large because they have either never been observed or observed with a large uncertainty. These uncertainties are defined in Table 6 for Mars and Table 7 for Mercury. C_{d0d0} is the observation covariance matrix and the parameter solution to the inverse problem is given by:

$$\hat{p} = C_{pp}^{-1} G^T C_{d0d0}^{-1} (d - Gp_0) + p_0, \quad (12)$$

where p_0 is the a priori parameter model and the functional G is defined by: $G_{ij} = \frac{\partial G_i}{\partial p_j}$. In our case, G_i corresponds to the total rotation matrix between the body-fixed and the inertial reference frame. We have chosen to suppose a uniform rotation model, meaning that the a priori rotation parameters p_0 are set to zero (see Tables 6 and 7). In our simulation, the observation data vector d has been constructed as follows: the ground tracks of the laser shots have been computed using a uniform rotation model for Mars and Mercury. Next the crossovers have been derived. The body-fixed positions of these crossovers define our a priori data Gp_0. The same ground crossovers have been converted to the J2000 inertial space using a uniform rotation model. These inertial crossing positions have been re-converted into the body-fixed reference frame using a non-uniform rotation model as defined in sections 3 and 4 for Mars and Mercury, respectively. These new body-fixed positions define our observation data containing the information we are interested in, i.e., the nutations and LOD variations for Mars or the librations and obliquity for Mercury. In reality, these data will be estimated from the crossovers determined as in the study by *Neumann et al.* [2001] that will be relocated to their actual position on the planet surface thanks to the azimuthal slopes and altimetry residuals and the static topography. This work will be carried out later with actual data sets as this article is devoted to the feasibility study only.

[28] Moreover, we suppose that the data covariance matrix is diagonal (we assume that there is no correlation between crossovers) where the diagonal values are the standard deviations of the observations. The results of the simulation are presented and discussed in the following section.

6. Discussion

[29] The altimetry crossover analysis leads to the Martian Orientation Parameters (MOP) summarized in Table 6 and to the Hermean Orientation Parameters (HOP) in Table 7. The HOP are perfectly recovered from the altimetry crossover inversion, while for Mars, only the main nutation amplitudes are recovered. No improvement has been obtained for the spin rate variations (LOD) from this altimetry crossover analysis.

[30] For Mars, the a posteriori covariance matrix represented in Figure 4b illustrates the strong correlation between the annual nutation amplitudes in longitude ψ_{10}, ψ_{40} as well as the correlation between the spin rate amplitudes. As a consequence, we will limit the inversion to a few parameters. As the rigid nutations of Mars are well known, we will try to recover only the nutation amplitudes that are most affected by the presence of a fluid core, i.e., the semi-annual and the ter-annual nutation amplitudes [*Dehant et al.*, 2000]. Therefore we retrieve only ψ_{50}, ψ_{60} and I_{50}, which have large amplitudes and are not correlated at all (Figure 4c). The inverted three MOP are represented in Figure 5 with the modeled values of section 3 attached with large a priori uncertainties as defined in Table 6. The error bars reflect the a posteriori formal error (1σ). Figure 4a shows that the a posteriori uncertainties of the parameters (e.g., here for ψ_{50} and I_{50}) are decreasing with the number of crossover points used in the inversion. The crossover distribution on Mars surface after seven Martian days of MGS mapping is also represented.

[31] Two crossover distributions have been simulated: (1) a 7-day crossing tracks on the whole surface of Mars leading to 5428 crossovers; (2) only a subset of 1114 crossovers identified in the Tharsis region. In both cases, the nutation amplitudes have been correctly retrieved with smaller uncertainties. Table 6 gives the a posteriori uncertainties and the estimated values for the MOP. *Yseboodt et al.* [2003] have shown that the perturbation due to the Free Core Nutation (FCN) is up to 12 mas, well below our a posteriori uncertainties. In the previous results, we have supposed an error of 100 m on each crossover observation. We can check the influence of the value of this error on the posterior uncertainties. For standard deviations of the observed crossover position taking respectively the values of 5, 10, 50, 100, 200 and 500 m, we have plotted the resulting posterior uncertainty on the three parameters in Figure 5c. Besides, we have considered two types of prior constraints: strong a priori constraints (a prior close to the modeled values $\psi_{50\ \text{a priori}}$ = 1089 ± 100 mas, $\psi_{60\ \text{a priori}}$ = 155 ± 100 mas and $I_{50\ \text{a priori}}$ = 514 ± 100 mas); weak a priori constraints (a null prior with large uncertainties of

Figure 4. (a) Crossover distribution during 7-day mapping of MGS and a posteriori standard deviation for ψ_{50} and I_{50} as a function of the number of crossover points used in the inversion scheme. (b) A posteriori covariance matrix for the 13 first parameters that are correlated. From left to right and from bottom to top, the parameters are, respectively: ψ_{10}, ψ_{20}, ψ_{40}, ψ_{50}, ψ_{60}, I_{00}, I_{10}, I_{20}, I_{40}, I_{50}, I_{60}, ϕ_{c1}, ϕ_{s1}, ϕ_{c2}, ϕ_{s2}. (c) A posteriori covariance matrix for the 3 nutation amplitudes that are finally investigated and their inter-correlation as function of the number of crossovers.

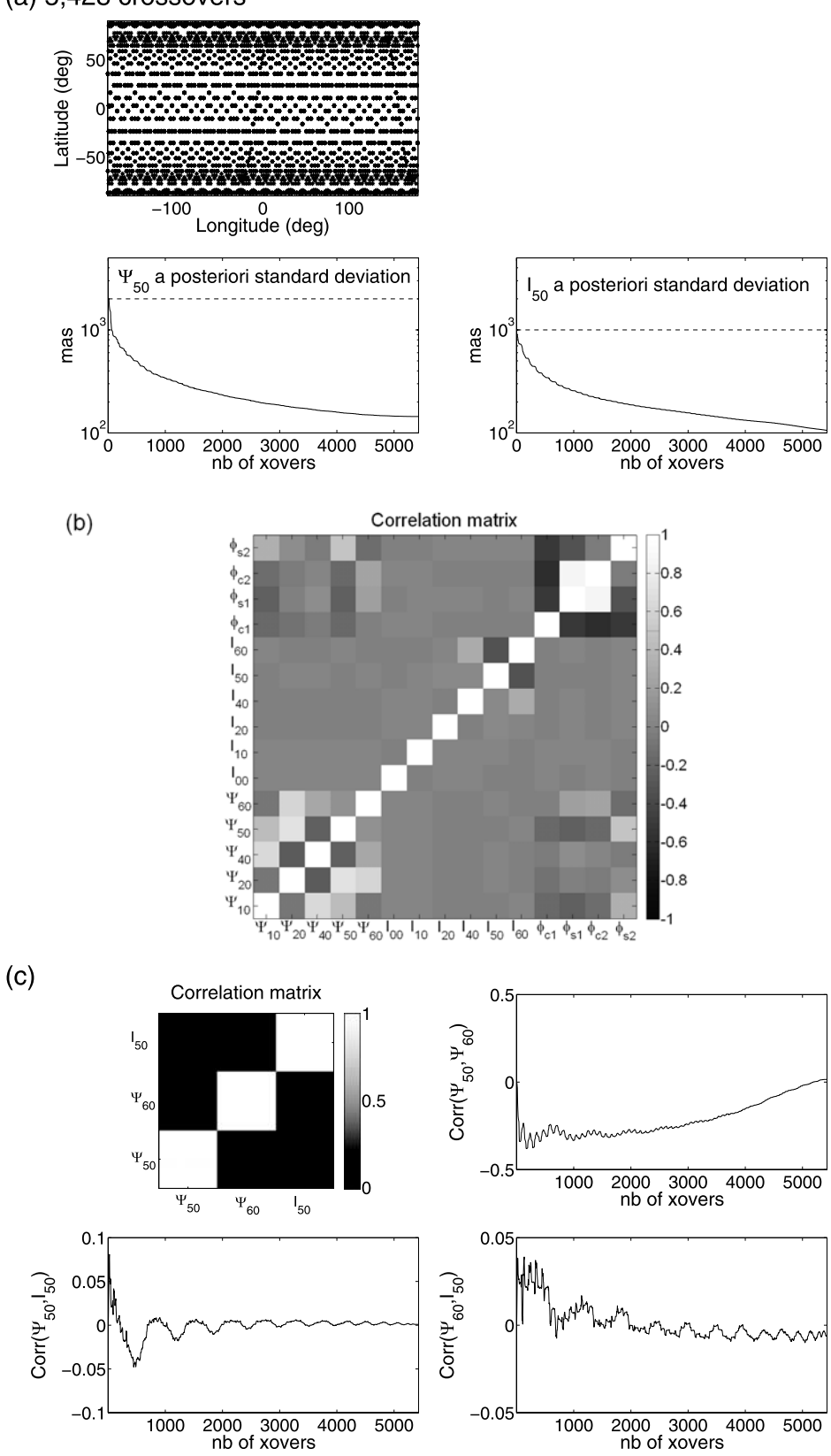
(a) 5,428 crossovers
Latitude (deg)
Longitude (deg)
Ψ50 a posteriori standard deviation
I50 a posteriori standard deviation
mas
nb of xovers
(b)
Correlation matrix
(c)
Correlation matrix
Corr(Ψ50,Ψ60)
Corr(Ψ50,I50)
Corr(Ψ60,I50)

Figure 4

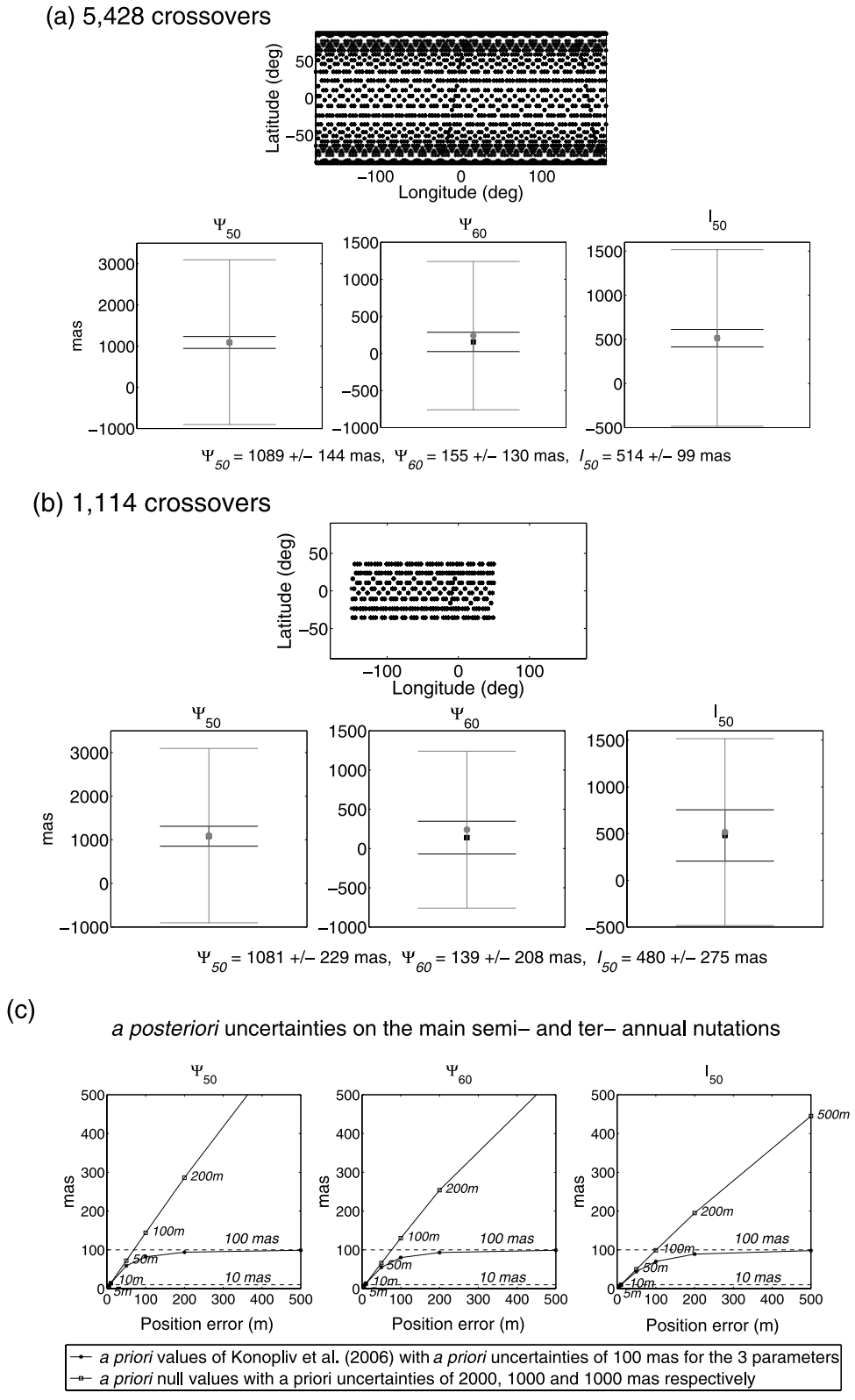

Figure 5. MOP inversion results for the main nutation amplitudes ψ_{50}, ψ_{60} and I_{50} using (a) 5428 crossovers uniformly distributed and (b) 1114 crossovers present in the Tharsis area. The retrieved MOP values are given below the graphs and are represented by the black squares while the modeled values are plotted in grey circles. (c) A posteriori uncertainties as function of the standard deviation on the crossover position, with and without strong prior constraints.

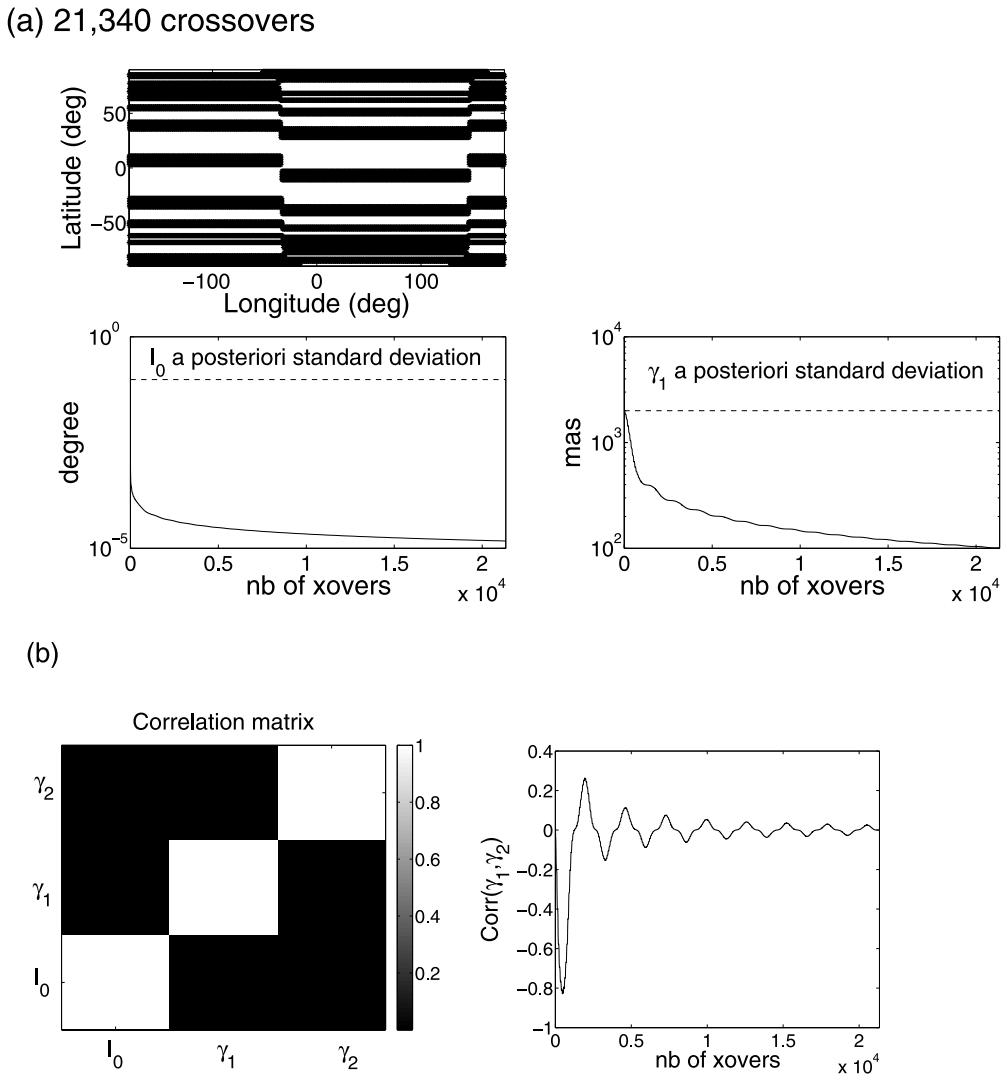

Figure 6. Crossover distribution during 1 Hermean day mapping of MPO around Mercury and a posteriori standard deviation for $\mathbf{I}_0$ and γ_1 as a function of the number of crossover points used in the inversion scheme. (b) a posteriori covariance matrix for the 3 HOP. From left to right and from bottom to top, the parameters are respectively: $\mathbf{I}_0$ and γ_1 γ_2. The correlation between γ_1 γ_2 is also plotted as a function of the number of crossovers used in the inversion.

2000 mas for ψ_{50} and of 1000 mas for ψ_{60} and I_{50}). We can see that in order to reach an uncertainty of 10 mas, and therefore to be able to detect the effect of the liquid core, we would need a positioning error of less than 10 m, even when imposing strong a priori constraints. Of course, we have considered here only 5428 crossovers obtained for a 7-day orbit of MGS; the actual MOLA data have been acquired for more than 2 years of mapping and would lead to several millions of crossovers [cf., *Neumann et al.*, 2001], which will contribute to a further decrease of the a posteriori uncertainty on the nutation amplitudes.

[32] The results obtained with this simulation show that it is possible to retrieve the amplitudes of the nutations from crossover data. However, even if the uncertainty on the results enable to obtain roughly the nutation amplitudes, it will not be possible to retrieve the contribution of a liquid core to these amplitudes, except if the FCN resonance period is right on the ter-annual (or quarter-annual). In that case, we might have a large enhancement of the nutation [see *Dehant et al.*, 2000; *Van Hoolst et al.*, 2000b] that will be above the observation uncertainties. For that resonance to happen, the dimension of the core would have to be very specific providing an FCN period equal or very close to the ter-annual nutation period (or to the quarter-annual nutation period). This could be the case for a large core (or extremely large core, resp.). However the amplitude of the nutation in that case would very much depend on the FCN quality factor (because of dissipation at the core-mantle boundary) in addition to the exact FCN period. There is a trade-off between the knowledge of the dissipation mechanism at the

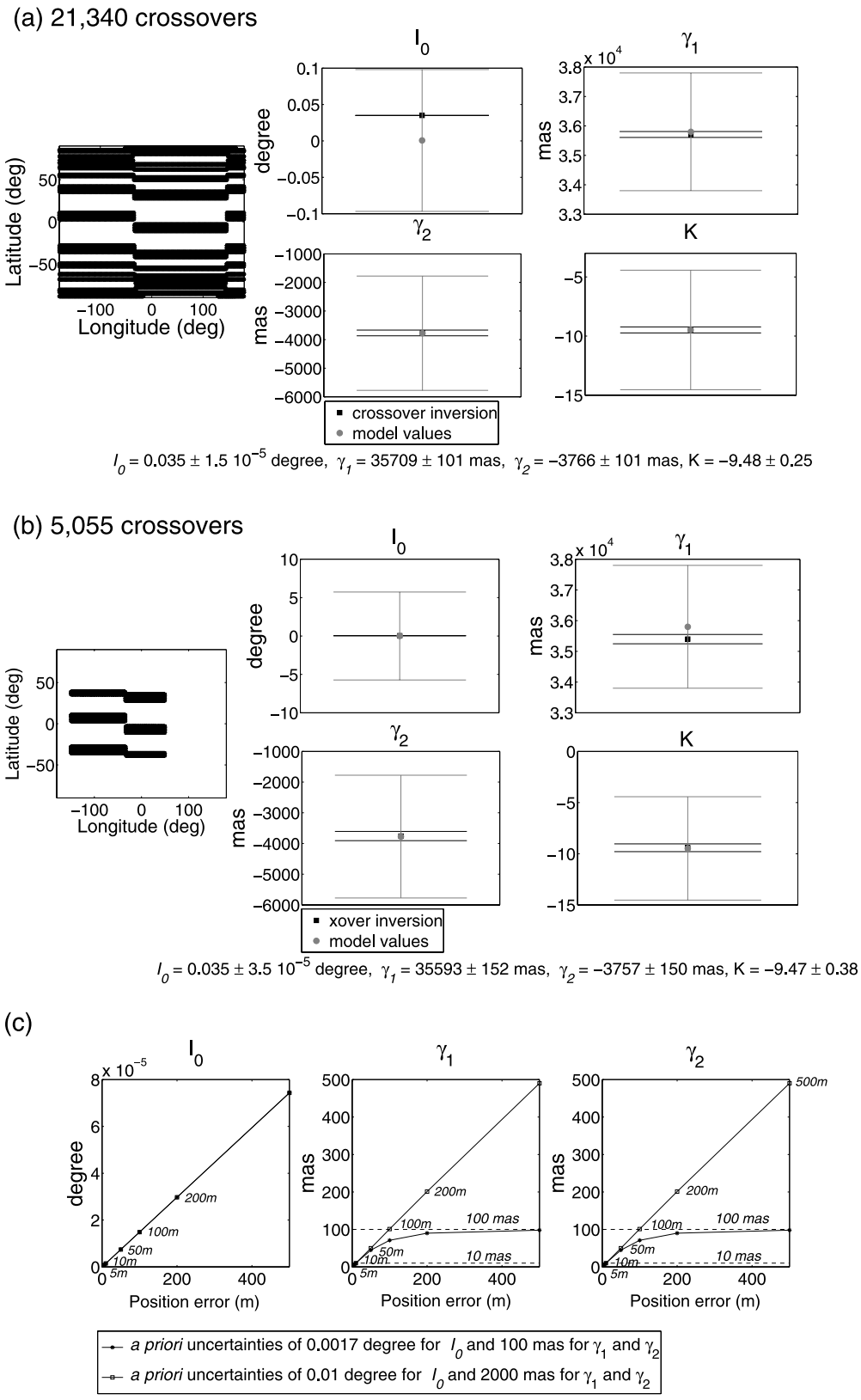

Figure 7. HOP inversion results using (a) 21,340 crossovers and (b) 5055 crossovers. The retrieved HOP values are given below the graphs and are represented by the black squares while the modeled values are plotted in grey circles. (c) A posteriori uncertainties as function of the standard deviation on the crossover position, with and without strong prior constraints.

core-mantle boundary and the dimension of the core. Dissipation is difficult to evaluate for Mars as it is very different from that of the Earth involving the magnetic field for nutation. The value of the k_2 tidal Love number determined by *Konopliv et al.* [2006] corresponds to a large core. This case is thus a possible situation in which the FCN may be detected.

[33] For Mercury, the BELA altimetry crossover inversion enables to retrieve the longitude libration amplitudes and the obliquity value (Table 7), despite the slow spin rate of Mercury and the poor coverage of the crossing points (Figure 6a). The three orientation parameters involved in the inversion are not correlated (Figure 6b). The obliquity and annual libration amplitude have a posteriori uncertainties decreasing considerably with the number of crossovers (Figure 6a). Two crossover distributions have been used: (1) a 1-day crossover set of 21,340 points; (2) a sub-set of 5055 crossovers located between $-40°$ and $40°$ in latitude, and between $-150°$ and $50°$ in longitude, as for the Tharsis area for Mars. The respective HOP inversion results are plotted in Figure 7a and Figure 7b. The modeled values as defined in section 4 with the a priori uncertainties defined in Table 7 are also plotted. We can see that even with fewer crossover points, we can retrieve the HOP within an accuracy of 100 mas for the librations and 0.001 arcmin for the obliquity. Therefore the observations made by *Margot et al.* [2007] could be verified and improved with the use of the future BELA altimetry crossovers. These results can be compared with those from a recent article of *Koch et al.* [2008]. These authors have simulated the libration and tidal effects on the altimetric signal and have shown that the amplitudes can only be retrieved with an accuracy of approximately 10%. They did not use the crossover information but rather used the direct effect of the libration on the altimetric distances.

[34] The influence of the standard deviation of each crossover position on the posterior uncertainties is plotted in Figure 7c. As for the MOP, two cases have been considered: strong a priori constraints (a prior based on the modeled values with small uncertainties, i.e., $I_{0\ \text{a priori}} = 0.035 \pm 0.0017°$, $\gamma_{1\ \text{a priori}} = 35{,}800 \pm 100$ mas and $\gamma_{2\ \text{a priori}} = -3775 \pm 100$ mas); weak a priori constraints (a null prior with large uncertainties of $0.01°$ for I_0 and of 2000 mas for γ_1 and γ_2). Note that for I_0, we obtain the same curve in both cases of a priori constraints. Even with large errors on the crossover positioning (e.g., 500 m), the posterior uncertainty on the obliquity is well below the 1σ-uncertainty obtained by *Margot et al.* [2007]. With weak a priori constraints, we can expect to reach an uncertainty of 100 mas for the Mercury libration amplitudes if the crossover positioning accuracy is 100 m.

7. Conclusion

[35] The simulations performed in this article show that altimetry crossover coordinates can be used to better constrain the rotation of Mars and Mercury. For Mars, only the main nutations can be retrieved with an improved uncertainty, while for Mercury both the obliquity and librations can be accurately estimated from the crossover points. Therefore we can expect to verify and improve the observations made by *Margot et al.* [2007] with the use of the future BELA altimetry ground track crossings. Our simulations have shown that the estimates of each Mars orientation parameter are strongly correlated and each parameter can be retrieved independently only through a compromise with their posterior uncertainty or with a priori constraints on their amplitudes from our knowledge of the rotation model. Indeed, the gravitational forcing from the Sun and the other planets is well known. The only unknown is the core contribution. This will only change the semi-annual prograde nutation at the percent level, the ter-annual retrograde nutation, and the quarter-annual retrograde nutation. Retrieving these three nutations only will help in the determination of the nutation amplitudes of Mars. If the core of Mars is large, the increase of two retrograde nutations could possibly be seen and could provide information on the core physical properties.

[36] The method is limited by the necessity to use topographic features in order to determine the actual crossover position independently of any rotation model, which makes this crossover analysis suitable only for planets with a sufficiently rough surface.

[37] In a future work, the application of the method to actual crossover points acquired during the mapping of the Mars Global Surveyor spacecraft with the MOLA laser altimeter will be performed. A following study could also be carried out based on the MESSENGER MLA instrument data from the orbital phase starting on 18 March 2011.

[38] **Acknowledgments.** This work was financially supported by the Belgian PRODEX program managed by the European Space Agency in collaboration with the Belgian Federal Science Policy Office. The authors thank T. Van Hoolst, who has greatly improved this manuscript for English and clarity. Many thanks also to G. Neumann and an anonymous reviewer for their useful comments on this work.

References

Anselmi, A., and G. E. N. Scoon (2001), BepiColombo, ESA's Mercury Cornerstone mission, *Planet. Space Sci.*, *49*, 1409–1420.

Balogh, A., and G. Giamperi (2002), Mercury: The planet and its orbit, *Rep. Prog. Phys.*, *65*, 529–560.

Dehant, V., P. Defraigne, and T. Van Hoolst (2000), Computation of Mars' transfer function for nutation, tides, and surface loading, *Phys. Earth Planet. Inter.*, *117*, 385–395.

Folkner, W. M., R. D. Kahn, R. A. Preston, C. F. Yoder, E. M. Standish, J. G. Williams, C. D. Edwards, R. W. Hellings, T. M. Eubanks, and B. G. Bills (1997), Mars dynamic from Earth-based tracking of the Mars Pathfinder Lander, *J. Geophys. Res.*, *102*, 4057–4064.

Harder, H., and G. Schubert (2001), Sulfur in Mercury's core?, *Icarus*, *151*, 118–122.

Jehn, R., C. Corral, and G. Giampieri (2004), Estimating Mercury's 88-day libration amplitude from orbit, *Planet. Space Sci.*, *52*, 727–732.

Kaula, W. M. (1966), *Theory of Satellite Geodesy. Applications of Satellite to Geodesy*, Blaisdell, Waltham, Mass.

Koch, C., U. Christensen, and R. Kallenbach (2008), Simultaneous determination of global topography, tidal Love number and libration amplitude of Mercury by Laser altimetry, *Planet. Space Sci.*, *56*(9), 1226–1237.

Konopliv, A. S., C. F. Yoder, E. M. Standish, D.-N. Yuan, and W. L. Sjogren (2006), A global solution for the Mars static and seasonal gravity, Mars orientation, Phobos and Deimos masses, and Mars ephemeris, *Icarus*, *182*, 23.

Margot, J. L., S. J. Peale, R. F. Jurgens, M. A. Slade, and I. V. Holin (2007), Large longitude libration of Mercury reveals a molten core, *Science*, *316*, 710–714.

Neumann, G. A., D. D. Rowlands, F. G. Lemoine, D. E. Smith, and M. T. Zuber (2001), Crossover analysis of Mars Orbiter Laser Altimeter data, *J. Geophys. Res.*, *106*(E10), 23,753–23,768.

Peale, S. J., R. J. Phillips, S. C. Solomon, D. E. Smith, and M. T. Zuber (2002), A procedure for determining the nature of Mercury's core, *Meteorit. Planet. Sci.*, *37*, 1269.

Rambaux, N., T. Van Hoolst, V. Dehant, and E. Bois (2007), Inertial core-mantle coupling and libration of Mercury, *Astron. Astrophys.*, AA3974-05.

Reasenberg, R. D., and R. W. King (1979), The rotation of Mars, *J. Geophys. Res.*, *84*, 6231–6240.
Roosbeek, F. (2000), Analytical developments of rigid Mars nutation and tide generating potential series, *Celest. Mech. Dyn. Astron.*, *75*, 287–300.
Rowlands, D. D., D. E. Pavlis, F. G. Lemoine, G. A. Neumann, and S. B. Luthcke (1999), The use of laser altimetry in the orbit and attitude determination of Mars Global Surveyor, *Geophys. Res. Lett.*, *26*, 1191–1194.
Seidelmann, P. K., et al. (2002), Report of the IAU/IAG Working Group on cartographic coordinates and rotational elements of the planets and satellites: 2000, *Celest. Mech. Dyn. Astron.*, *82*(1), 83–111.
Smith, D. E., et al. (1999), The global topography of Mars and implications for surface evolution, *Science*, *284*, 1495–1503.
Solomon, S. C., R. L. McNutt, R. E. Gold Jr., and D. L. Domingue (2007), MESSENGER mission overview, *Space Sci. Rev.*, *131*, 3–39.
Tarantola, A., and B. Valette (1982), Generalized nonlinear inverse problems solved using the least squares criterion, *Rev. Geophys.*, *20*, 219–232.
Thomas, N., et al. (2007), The BepiColombo Laser Altimeter (BELA): Concept and baseline design, *Planet. Space Sci.*, *55*, 1398–1413.
Trinh, A. (2007), Effet des marées de Mercure sur les mesures altimétriques de la mission spatiale BepiColombo, mémoire de licence, ULB, Bruxelles, Belgium.
Van den Acker, E., T. Van Hoolst, O. de Viron, P. Defraigne, F. Forget, F. Hourdin, and V. Dehant (2002), Influence of the seasonal winds and the CO_2 mass exchange between atmosphere and polar caps on Mars' rotation, *J. Geophys. Res.*, *107*(E7), 5055, doi:10.1029/2000JE001539.
Van Hoolst, T., V. Dehant, and P. Defraigne (2000a), Chandler wobble and free core nutation for Mars, *Planet. Space Sci.*, *48*, 1145–1151.
Van Hoolst, T., V. Dehant, and P. Defraigne (2000b), Sensitivity of the free core nutation and the Chandler Wobble to changes in the interior structure of Mars, *Phys. Earth Planet. Inter.*, *117*, 397–405.
Yseboodt, M., and J.-L. Margot (2006), Evolution of Mercury's obliquity, *Icarus*, *181*, 327–337.
Yseboodt, M., J.-P. Barriot, and V. Dehant (2003), Analytical modeling of the Doppler tracking between a lander and a Mars orbiter in terms of rotational dynamics, *J. Geophys. Res.*, *108*(E7), 5076, doi:10.1029/2003JE002045.
Zuber, M. T., T. E. Smith, S. C. Solomon, D. O. Muhleman, J. W. Head, J. B. Garvin, J. B. Abshire, and J. L. Bufton (1992), The Mars Observer laser altimeter investigation, *J. Geophys. Res.*, *97*, 7781–7797.

V. Dehant, P. Rosenblatt, and A. Trinh, Department Reference Systems and Geodynamics, Royal Observatory of Belgium, Ave. Circulaire, 3, B-1180 Brussels, Belgium.

S. Rosat, Ecole et Observatoire des Sciences de la Terre-Institut de Physique du Globe de Strasbourg, UMR7516, 5 rue Descartes, 67084 Strasbourg, Cedex, France. (severine.rosat@eost.u-strasbg.fr)